ELSEVIER

Journal of Molecular Catalysis A: Chemical 186 (2002) 153–161

JOURNAL OF MOLECULAR CATALYSIS A: CHEMICAL

www.elsevier.com/locate/molcata

Hydrogenolysis of 1,1a,6,10b-tetrahydro-1,6-methanodibenzo [*a*,*e*]cyclopropa[*c*]-cycloheptene over silica- and zirconia-embedded Ru-colloids

Simona Oprescu [a], Viorica Pârvulescu [b], Aurica Petride [c], Mircea D. Banciu [d], Vasile I. Pârvulescu [a,*]

[a] *Department of Catalysis, Faculty of Chemistry, University of Bucharest, B-dul Regina Elisabeta 4-12, Bucharest 70346, Romania*
[b] *Institute of Physical Chemistry of Romanian Academy of Science, Splailul Independentei 212, Bucharest, Romania*
[c] *Center of Organic Chemistry, Splaiul Independentei 202b, 71141 Bucharest, P.O. Box 15-258, Romania*
[d] *Department of Organic Chemistry, Polytechnic University Bucharest, Splaiul Independentei 313, Bucharest, Romania*

Received 19 March 2000; accepted 28 November 2001

Abstract

Hydrogenolysis of 1,1a,6,10b-tetrahydro-1,6-methanodibenzo[*a*,*e*]cyclopropa[*c*]-cycloheptene over Ru-embedded colloids is reported. The preparation of the catalysts was made by embedding pre-synthesized Ru-stabilized colloids in a zirconia or silica sol–gel matrix. $N^+(C_8H_{17})_4Br^-$ and $N^+(CH_3)_3C_{16}H_{33}Br^-$ were used as stabilizers. The catalysts were characterized by adsorption–desorption isotherms of N_2 at 77 K, H_2-chemisorption, XRD, small angle scattering (SAXS) and XPS. The reaction was found to be mainly influenced by the catalysts characteristics (nature of the inorganic matrix and metal dispersion) and by the reaction conditions (merely the temperature and the solvent). The first step, namely the fission of the cyclopropane ring, proceeds regioselectively.

Keywords: 1,1a,6,10b-Tetrahydro-1,6-methanodibenzo[*a*,*e*]cyclopropa[*c*]-cycloheptene; Colloids; Heterogeneous catalysts; Hydrogenolysis

1. Introduction

Catalytic hydrogenolysis of C–C bonds is generally investigated either in relation with the stability of the reforming catalysts or with the transformation of the large aromatic molecules into smaller ones [1–3]. It involves the rupture of a carbon–carbon bond via interaction with hydrogen. Such reactions are controlled by radical mechanisms which are associated with a relatively low selectivity of the reaction products [4]. In addition, in most cases the reaction is accompanied by secondary homologation processes, which lead to the formation of coke and finally to the catalyst deactivation. The hydrogenolysis is very sensible to the various changes of the catalyst and, therefore, is suitable for the characterization of many catalysts [5]. For Ru, it is well known that large metal particles lead to an advanced rupture [6]. Studies of the hydrogenolysis of cycloalkanes have been mainly limited to 3- to 6-member carbocycles, when aromatization, rearrangement with dehydrocyclization, and multiple carbon–carbon bond cleavages were observed [7].

Nowadays, the heterogeneous catalysts which have been investigated in hydrogenolysis reactions were obtained using impregnation techniques [8–12]. Even for the very well controlled preparations, these techniques lead to metal supported catalysts with a dispersion

* Corresponding author.
E-mail address: v_parvulescu@chim.upb.ro (V.I. Pârvulescu).

1381-1169/02/$ – see front matter
PII: S1381-1169(02)00072-9

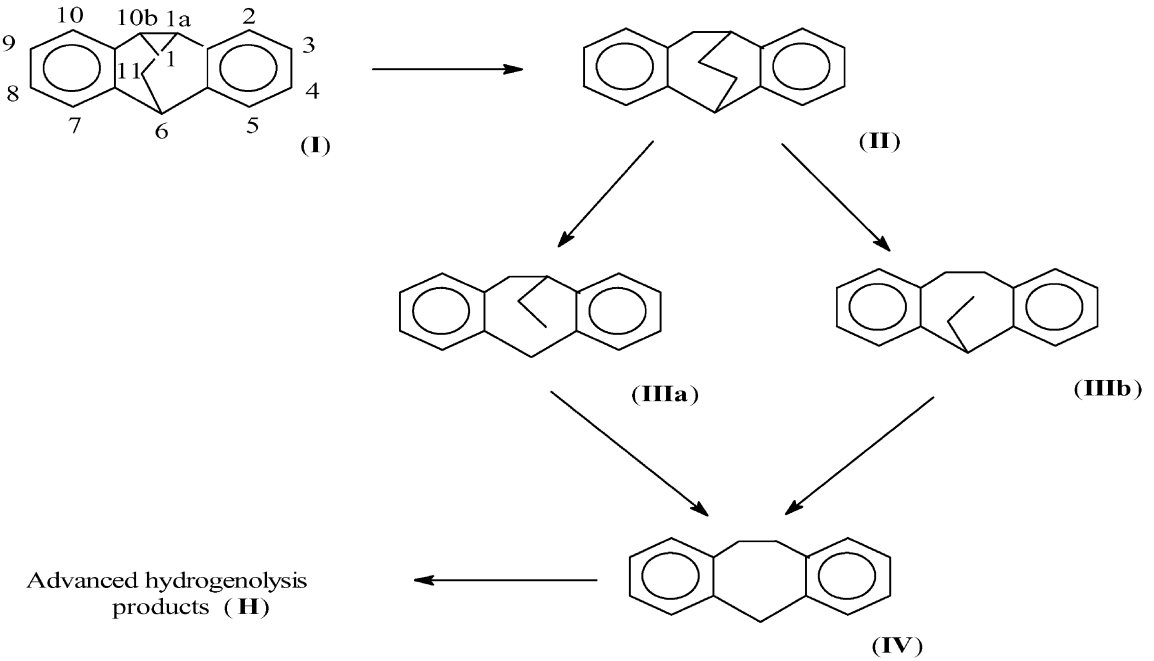

Scheme 1. Reaction pathways in hydrogenolysis of (**I**).

of particle sizes [13,14]. The use of pre-synthesized stabilized colloids with very well controlled dimensions, instead of the impregnated catalysts, could give very valuable information about the relation particle size-activity.

The aim of this paper is to present the results obtained in the selective hydrogenolysis of 1,1a,6,10b-tetrahydro-1,6-methanodibenzo[*a*,*e*]cyclopropa[*c*]-cycloheptene (**I**) to 5*H*-10,11-dihydro-5,11-ethanodibenzo[*a*,*d*]cycloheptene (**II**) and the accompanying processes occurring using silica- or zirconia-embedded Ru-colloids. The hydrocarbon (**I**) synthesized by our group [15] is a symmetrical strained polycyclic compound including different reaction sites active during catalytic hydrogenation. The hydrogenolysis of (**I**) may follow the routes described in Scheme 1. Therefore, the selectivity of this reaction was another item followed in this study. The aim was to stop the hydrogenolysis at the level of compound (**IV**). Derivatives of (**IV**) exhibit biological activity. One example is the well known drug Elavil [16].

2. Experimental

2.1. Catalyst preparation

Quaternary-ammonium salts-stabilized-Ru-colloids were obtained using a reported procedure [17,18], using $N^+(C_8H_{17})_4Br^-$ (TOAB) and $N^+(CH_3)_3C_{16}H_{33}Br^-$ (TMCB) as stabilizers. Accordingly, 39.5 mmol anhydrous $RuCl_3$ were dissolved in 500 anhydrous THF and reduced with $N(C_8H_{17})_4BEt_3H$ or $N(C_6H_{33})(CH_3)_3BEt_3H$ in a molar ratio reductant: Ru = 3:1. The size of the colloids was 9 nm for those prepared with TMCB, and 6 nm for those prepared with TOAB, respectively. These materials showed an excellent stability in THF. The colloids as prepared were embedded in a zirconia (samples Ru-Zr-TOAB and Ru-Zr-TMCB) or silica sol–gel matrix (samples Ru-Si-TOAB and Ru-TMCB) using the procedure reported elsewhere [19]. According to this method, the Ru-colloids were added in the oxide gelation step. Tetraethoxisilicate (TEOS) was used as the precursor for the silica support. However, since the

NR_4-stabilized-Ru-colloids are completely insoluble and even decompose at elevated temperatures in alcoholic solutions, the normal sol–gel procedure has to be modified using THF as the solvent. The molar composition of the sol was TEOS:THF:H_2O:HCl = 1:3.5:4:0.05. The colloid was added as a 4.5 wt.% THF-solution at room temperature, after refluxing. The sol was stirred vigorously at 70 °C (under reflux) until the gelification was complete (after 2 days). To avoid any decomposition in the presence of air, all steps were carried out under Ar. The resulting gel was dried under vacuum at 110 °C using a ramp of 0.12 °C min^{-1}. For zirconia, the gel was obtained using zirconium propoxide (ZP, Aldrich) as precursor. Hydrolysis of ZP was carried out in the presence of acetic acid and the molar composition of the sol was ZP:THF:H_2O:CH_3COOH = 1:3.5:4:0.05. Samples with 2 wt.% Ru were prepared.

For comparison, pure ZrO_2 and SiO_2 samples were obtained following the same procedure.

2.2. Surface area measurements

The sorption isotherms of N_2 at 77 K were obtained with a Micromeritics ASAP 2000 apparatus after outgassing the samples at 393 K for 24 h under vacuum.

2.3. Hydrogen chemisorption

H_2-chemisorption measurements were carried out using a Micromeritics ASAP 2010C apparatus. The samples were evacuated at 403 K for 36 h. Soon after, a hydrogen flow was passed initially at 308 K for 15 min, then the temperature was increased at 403 K at a heating rate of 5 K min^{-1} and maintained for 2 h. After reduction, the samples were purged with a helium flow at 403 K for 2 h and then at 308 K for another 30 min. The amounts of chemisorbed hydrogen were measured at 308 K by the desorption method after equilibration for 45 min in 300 Torr of adsorbate. The total hydrogen uptake was determined by extrapolating the linear portion of the adsorption isotherm to zero pressure. Reversible H_2-sorption was measured by outgassing at 5×10^{-5} Torr at the adsorption temperature and running a second isotherm. The difference between the total and reversible uptakes was ascribed to irreversible hydrogen. The ruthenium dispersion, surface area and particle size were determined from the irreversible uptake, assuming a H:Ru stoichiometry of 1 [20,21].

2.4. XPS measurements

The XPS spectra were recorded using a SSI X probe FISONS spectrometer (SSX-100/206) with monochromated Al Kα radiation. The spectrometer energy scale was calibrated using the Au $4f_{7/2}$ peak (binding energy 84.0 eV). For the calculation of the binding energies, the C 1s peak of the C–(C,H) component of adventitious carbon at 284.8 eV was used as an internal standard. In order to limit reoxidation, the reduced samples were transferred from the reduction set-up to the XPS apparatus under isooctane. The peaks assigned to Ru $3p_{3/2}$ and Ru $3d_{5/2}$, Si 2p, Zr $3d_5$ and O 1s levels were analyzed. No peak due to any chlorine component has been identified.

2.5. XRD and small angle scattering (SAXS)

The XRD patterns were recorded with a PW1050 diffractometer equipped with a secondary graphite monochromator. The Cu Kα radiation corresponds to λ = 1.54183 Å. The instrument used for SAXS was a STOE small angle attachment using a Kratky-collimator with 0.05 slit width and a sample detector distance of 300 mm. The detection of scattered X-rays was done via a stationary 4° position sensitive detector (PSD). The sample was rotated during the measurement and the beam path was in a helium atmosphere during measurement with graphite monochromated Cu Kα radiation (λ = 1.54183 Å).

2.6. Activity tests

Standard experiments used 10 mg (**I**) dissolved in 15 ml methanol or 2-propanol and 50 mg catalyst. The reaction was carried out in a stainless steel stirred autoclave at pressures between 4 and 10 atm, and temperatures between 60 and 100 °C. Prior to the catalytic tests the catalysts were treated in 15 ml solvent at 100 °C for 4 h under vigorous stirring. The reaction products were collected each 15 min till 4 h. The products were analyzed by GC using a Carlo Erba instrument (HRGC 5300 Mega Series) equipped with a fused silica capillary column of 25 m long and 0.32 mm inner diameter. The identification of the peaks was made using

pure synthesized compounds [22] which purity was checked by ^{1}H and ^{13}C NMR using a Varian Gemini 300BB instrument, operated at 300 MHz for ^{1}H and 75 MHz for ^{13}C.

3. Results

3.1. Surface area measurements

The textural characteristics of the investigated samples are given in Table 1. The catalysts containing zirconia showed surface areas smaller than those containing silica. The nature of the template used for the stabilization of colloids has also an influence upon the surface areas. The samples containing $N^{+}(CH_3)_3C_{16}H_{33}Br^{-}$ as stabilizing agent for colloid (samples denoted TMCB) showed higher surface areas than those containing $N^{+}(C_8H_{17})_4Br^{-}$ as stabilizing agent (samples denoted TOAB). All the investigated catalysts exhibited a mesoporous texture with a monomodal pore distribution. The pore size was determined only by the nature of the stabilizing agent. The samples prepared using $N^{+}(CH_3)_3C_{16}H_{33}Br^{-}$ had pores of about 2.5 nm, whereas those prepared with $N^{+}(C_8H_{17})_4Br^{-}$ had larger pores, i.e. of 4.1–4.3 nm. However, it is hard to explain the correlation between the surface area, pore diameters and the stabilizer used. The texture of these materials does not correspond to that of the oxides prepared using templates in which the template is decomposed during the calcination. The samples were only dried and the stabilizer still surrounds the colloids.

3.2. Hydrogen chemisorption

The H_2-chemisorption data are compiled in the same Table 1. The size of the ruthenium particles depended on the nature of the stabilizer and it was close to the size of the colloids before the embedding in the oxide matrix. The pure colloid prepared using $N^{+}(CH_3)_3C_{16}H_{33}Br^{-}$ had sizes very well centered at about 9 nm, whereas that prepared with $N^{+}(C_8H_{17})_4Br^{-}$ had smaller sizes, i.e. around 6 nm. These data come to confirm that the way in which the embedding of the colloids was carried out produced no damages in their integrity.

3.3. XRD and SAXS

Fig. 1 shows the XRD patterns of Ru-Si-TOAB catalyst. For comparison, the typical lines of SiO_2 and crystalline Ru are also given. Based on these data one can surely assign the broad peak centered at 2θ 21.83 to SiO_2. But the peaks located at 2θ 28.3, 40.5, 50.2, 58.7, 66.4, 70.5, and 73.7 do not correspond with the peaks of Ru (ASTM 6-653). These data show that the atomic arrangements in Ru-colloids are different of those in metallic ruthenium. The diffraction maxima of the colloidal Ru correspond to a cubic structure with the lattice parameter $a = 3.154$ Å. This indicates an interatomic distance of 3.154 Å in the colloidal state, instead of 2.65 Å in the bulk metal (ASTM 6-653). The patterns of the other investigated samples exhibited the same location of the peaks due to Ru-colloids. It is worth noting that the patterns of pure colloids showed peaks in the same position as in the embedded catalysts, which may be an additional evidence of the conservation of their structure.

The only difference between Ru-Zr-TOAB and Ru-Zr-TMCB, and Ru-Si-TOAB and Ru-Si-TMCB results from the location of the peak corresponding to the support. For the ZrO_2 containing catalysts the broad peak was located at 2θ 30.64.

Fig. 2 shows the SAXS pattern recorded for the same Ru-Si-TOAB catalyst. The peak located at 2θ

Table 1
Properties of the investigated catalysts

Property	Catalyst			
	Ru-Zr-TOAB	Ru-Zr-TMCM	Ru-Si-TOAB	Ru-Si-TMCB
Surface area ($m^2\,g^{-1}$)	94	72	165	102
Pore diameter (nm)	2.6	4.3	2.3	4.0
H_2 uptake ($cm^3\,g^{-1}$)	0.1643	0.2138	0.1622	0.2514
Dispersion (%)	15.2	19.2	14.6	22.6
Particle size (nm)	8.8	6.9	9.1	5.9

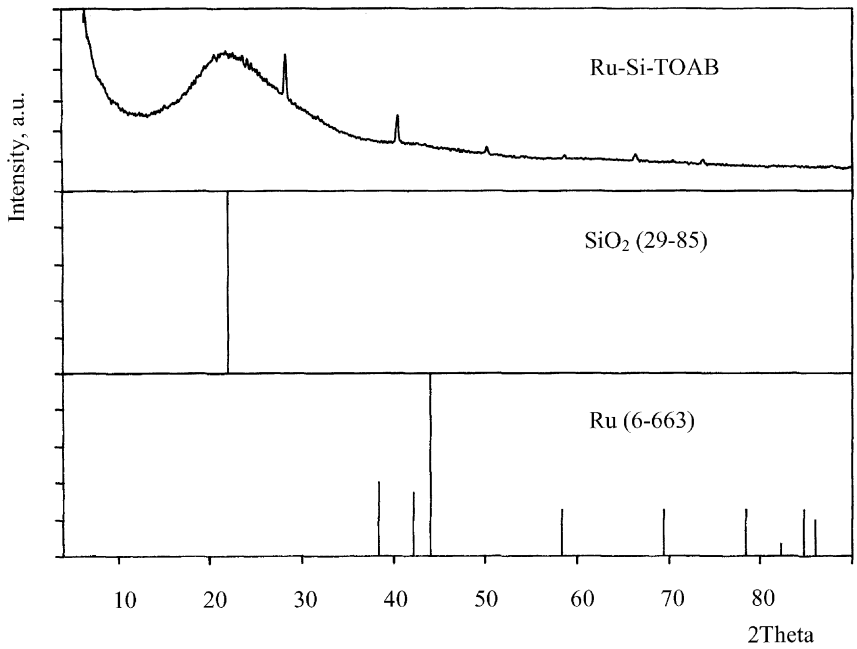

Fig. 1. XRD pattern of Ru-Si-TOAB.

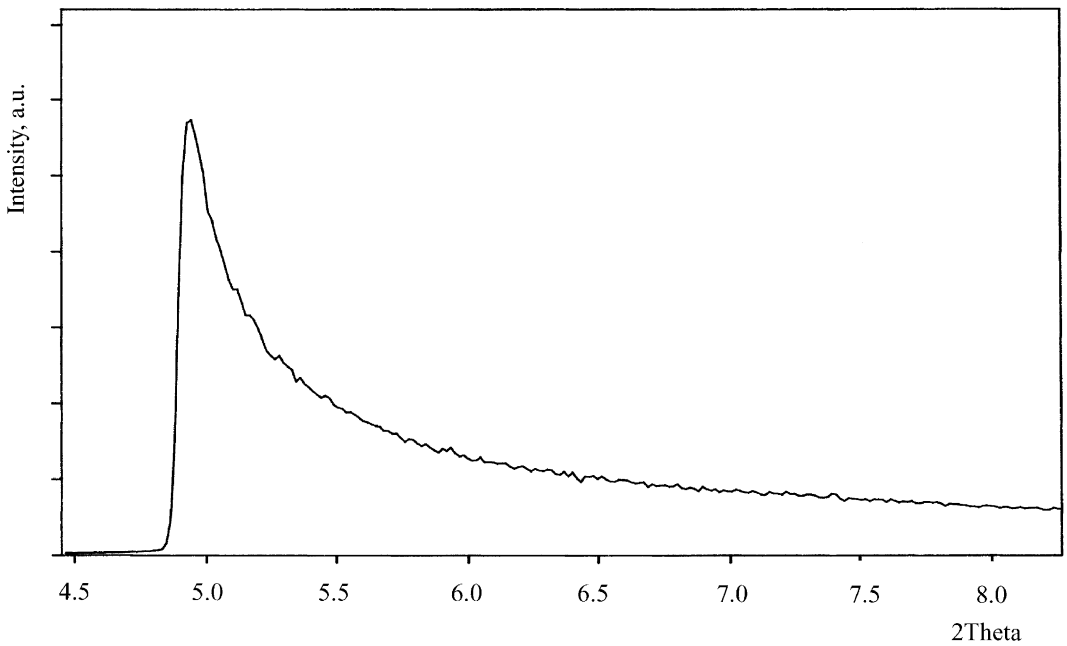

Fig. 2. SAXS pattern of Ru-Si-TOAB.

5.1 corresponds to a pore diameter of about 2 nm, as resulted from the application of the Bragg's rule. This demonstrates a good concordance with the results of adsorption–desorption of nitrogen at 77 K. The same concordance was determined for the other catalysts.

The continuous decay of the SAXS curve indicated a different texture than that of M41S materials. This may correspond to pores which exhibit a certain tortuosity and are randomly distributed. Debye et al. [23] have demonstrated that if the porosity is randomly distributed, the SAXS diffusion must follow a $1/(1 + b\theta^2 a^2)^2$ law, where "b" is a constant, "θ" the scattering angle and "a" is a correlation distance. By using this, we may obtain a correlation factor, a, that gives the confidence in the pore size. The treatment of the SAXS results by using this law led to values in the range "pore size ±5 Å", thus indicating again a good concordance with results obtained from adsorption–desorption isotherms.

3.4. XPS

Binding energies of Ru $3p_{3/2}$ component for all the investigated catalysts were in the range 461.4–461.6 eV, which correspond to reduced metal species [24]. These data gave additional evidence on the fact that the conditions in which the embedding took place caused no oxidation of the colloids. This may also be a confirmation of the role played by the protecting shell in this process.

Table 2
Conversion (%) of (**I**) at different temperatures over the investigated catalysts

Catalyst	2-Propanol			Methanol	
	60 °C	80 °C	100 °C	60 °C	80 °C
Ru-Zr-TOAB	48.4	49.3	51.2	9.8	10.6
Ru-Zr-TMCB	81.4	85.6			
Ru-Si-TOAB	86.8	90.2			
Ru-Si-TMCB		76.2	88.9		

3.5. Activity tests

Table 2 compiles the conversion of (**I**) over the different catalysts. The increase of the temperature leads to an increase of the conversion. Under the investigated conditions, Ru-Zr-TOAB exhibits the smaller conversions, and Ru-Si-TOAB and Ru-Si-TMCB the higher ones. Catalytic tests performed over the carriers prepared following the same procedure but without Ru showed no conversion.

Fig. 3 shows the variation of the product distribution on Ru-Zr-TOAB and Ru-Si-TMCB catalysts in 2-propanol. The hydrogenolysis merely stops at molecules (**II**)–(**IV**), irrespective of the temperature.

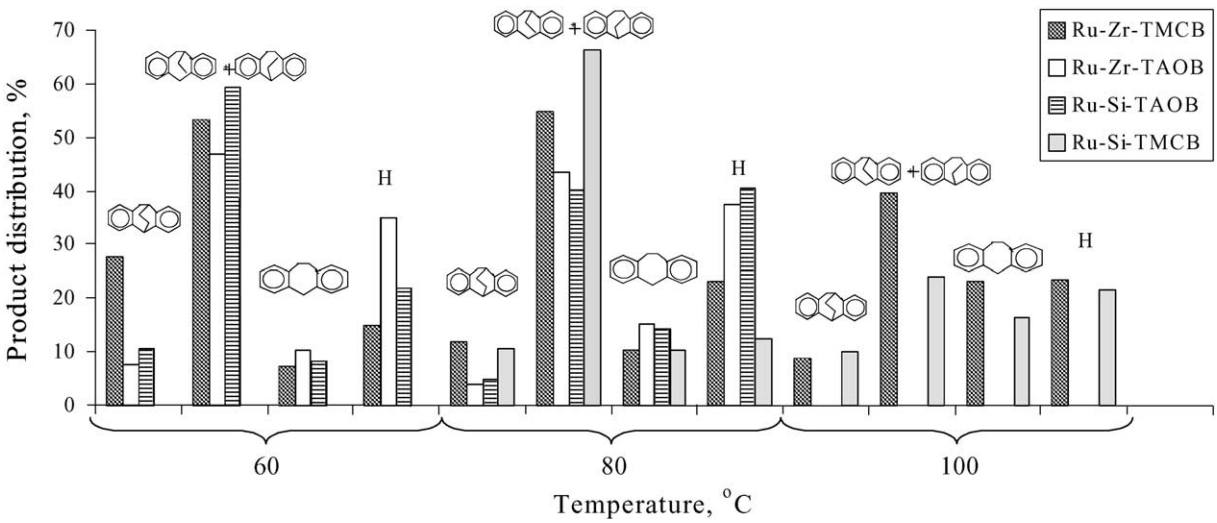

Fig. 3. Modification of the product distribution as a function of the catalyst and temperature (10 ml 2-propanol, 8 atm H_2, 4 h, 50 mg catalyst, 30 mg substrate).

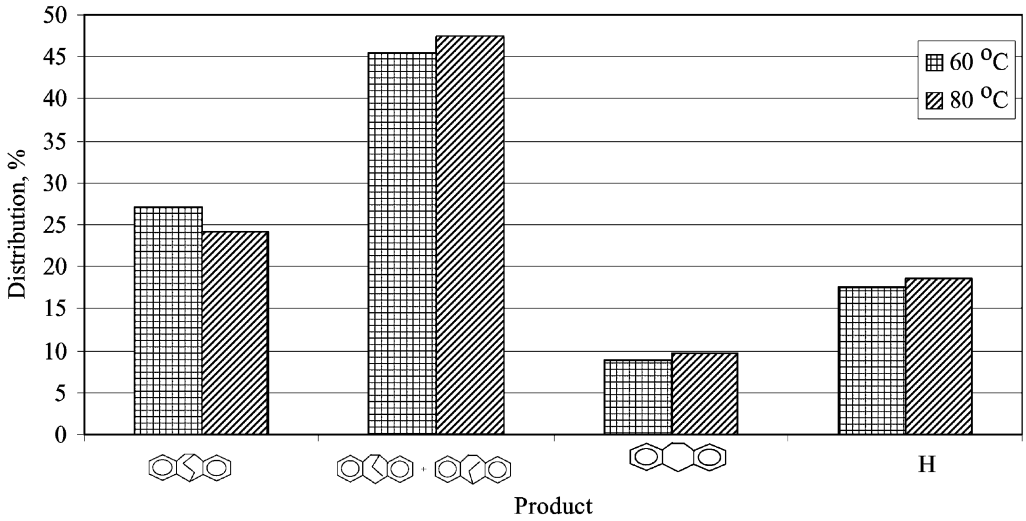

Fig. 4. Product distribution as function of the temperature on Ru-Zr-TOAB (10 ml methanol, 8 atm H_2, 4 h, 50 mg catalyst, 30 mg substrate).

On the other two catalysts, the hydrogenolysis goes further, with the seven rings being broken. Once the seventh ring is broken, the process becomes more complex and the resulting fragments undergo hydrogenolysis, hydrogenation and polymerization to heavy aromatics. All these compounds are denoted as H.

The conversions obtained in methanol are smaller than when using 2-propanol (Table 2) indicating a solvent effect. However, the selectivities remain still good under these conditions, the rupture of the seven rings being less than 20% (Fig. 4).

The influence of the pressure on the catalytic performances is illustrated in Fig. 5 for the Ru-Zr-TOAB catalyst. The increase of the H_2 pressure from 4 to 10 atm only causes a slight increase of the conversion. But the increase of the pressure in this range brings about a change of the product distribution. Higher pressures favor the formation of compound (**III**). The

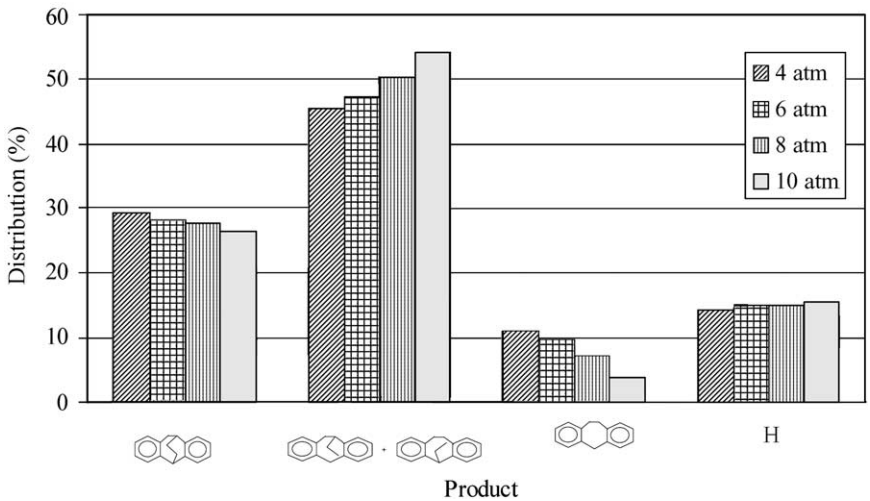

Fig. 5. Product distribution vs. pressure on Ru-Zr-TOAB (10 ml 2-propanol, 60 °C, 4 h, 50 mg catalyst, 30 mg substrate).

same increase of pressure has almost no influence on the advanced disruption and degradation to **H** species.

4. Discussion

The embedding of the ruthenium stabilized colloids in a sol–gel matrix like silica or zirconia was found to result in solid catalysts in which the size and the oxidation state of the colloid were preserved. XRD and XPS measurements gave evidences for such a behavior. The size of the Ru-colloids, as this was determined from H_2-chemisorption data, was in very good concordance with that of the initial colloids thus confirming the stability and the integrity of the colloids during the embedding process. The colloid stabilized with $N^+(C_8H_{17})_4Br^-$ had a smaller size (6 nm) than that stabilized with $N^+(CH_3)_3C_{16}H_{33}Br^-$ (around 9 nm).

The stabilizer also influenced the textural properties of the catalysts. The catalysts prepared using $N^+(CH_3)_3C_{16}H_{33}Br^-$ exhibited higher surface areas and smaller pores than those prepared with $N^+(C_8H_{17})_4Br^-$. The nature of the support was another factor influencing the textural characteristics. The SiO_2 containing catalysts showed larger surface areas and slightly smaller pores than ZrO_2 ones.

The catalytic results obtained with these materials suggest that the conversion of molecule (**I**) is influenced by the support nature. The Ru-colloids embedded in a silica matrix exhibit higher conversion than those embedded in a zirconia matrix. This difference could be related with the more basic character of zirconia which may interact with the delocalized π-electrons of the aromatic rings.

The selectivity of the reaction can be associated with the metal particle size exposed to the reactants. The best selectivities were obtained over the catalysts Ru-Zr-TMCB and Ru-Si-TMCB which, as shown by the chemisorption measurements, exhibited the highest dispersions. Based on these results, one can expect that higher metal particles allow a better interaction with molecule (**I**), finally leading to an advanced destruction, namely, to an increased content of **H** species. Such a behavior supports the previous data showing that large ruthenium ensembles afford an advanced rupture of C–C bonds [6] and is in agreement with the fact that hydrogenolysis is a structural sensitive reaction [5]. To make clearer the structural sensitive character, it should be underlined that the first step of hydrogenolysis of (**I**), namely, the breakage of the strained cyclopropane moiety, occurs regioselectively: Only the identical C1–C1a and/or C1–C10b bonds are hydrogenated, affording the product (**II**), whereas the C1a–C10b bond is not affected. This behavior can be ascribed to the fact that the C1–H bond being the most unhindered cyclopropanic one (as stereomodels show), it is easily fixed on the catalyst affording then the corresponding product (**II**).

The effect of the solvent is evident. The conversions obtained in methanol were smaller than when using 2-propanol (Table 2). This result can also be associated with the surface properties of the support and with the acidic character of methanol, suggesting a competition between the solvents and the reactant for the surface. The pretty good selectivity measured under these conditions (Fig. 4) can therefore be associated both with the solvent and particle size effect.

5. Conclusions

Hydrogenolysis of (**I**) on zirconia- and silica-embedded Ru-colloids is a stepwise process. The first step, fission of strained cyclopropanic ring proceeds regioselectively by the breaking of one of the two identical C1–C1a or C1–C10b bonds, leading to the ethano-bridged hydrocarbon (**II**). Further hydrogenolysis leads to unbridged dibenzocycloheptenic hydrocarbon (**IV**) via intermediates (**IIIA**) and (**IIIB**). Advanced hydrogenolysis conducts to heavy aromatic hydrocarbons (**H**). The product distribution was influenced by the catalysts characteristics (nature of the support and exposed particle metal size), and by the reaction conditions. Among those, temperature and solvent seem to be the most effective factors.

Acknowledgements

The authors kindly acknowledge Prof. Dr. Helmut Bönnemann from Max-Planck-Institut für Kohlenforschung, Abt. Heterogene Katalyse, Mülheim an der Ruhr,Germany for supplying Ru-colloids and for very useful discussions.

References

[1] J.H. Sinfelt, Catal. Rev. 3 (1969) 175.
[2] J.H. Sinfelt, J.L. Carter, D.J.C. Yates, J. Catal. 24 (1972) 283.
[3] G.C. Bond, Chem. Soc. Rev. 20 (1991) 441.
[4] G.C. Bond, J.C. Slaa, J. Mol. Catal. Chem. Technol. Biotechnol. 65 (1996) 15.
[5] I. Alstrup, U.E. Petersen, J.R. Rostrup-Nielsen, J. Catal. 191 (2000) 401.
[6] V. Ponec, G.C. Bond, Catalysis by Metals and Alloys, Elsevier, Amsterdam, 1995, p. 284.
[7] F. Locatelli, J.-P. Candy, B. Didillon, G.P. Nicolai, D. Uzio, J.-M. Basset, J. Am. Chem. Soc. 123 (2001) 1658.
[8] B. Torok, I. Palinko, A. Molnar, M. Bartok, J. Catal. 143 (1993) 111.
[9] G.C. Bond, A. Donato, J. Chem. Soc., Faraday Trans. 89 (1993) 3129.
[10] S. Kawi, J.-R. Chang, B. Gates, J. Phys. Chem. 98 (1994) 12978.
[11] F.B. Passos, M. Schmal, M.A. Vannice, J. Catal. 160 (1996) 106.
[12] R. Brown, Ch. Kemball, J. Chem. Soc., Faraday Trans. 92 (1996) 281.
[13] I.H. Cho, S.J. Cho, S.B. Park, R. Ryoo, J. Catal. 153 (1995) 232.
[14] G.C. Bond, J.C. Slaa, J. Chem. Technol. Biotechnol. 65 (1996) 15.
[15] E. Cioranescu, M.D. Banciu, R. Jelescu, M. Rentea, M. Elian, C.D. Nenitzescu, Tetrahedron Lett. (1969) 1871.
[16] M. Protiva, V. Hnevsova, M. Seidova, J. Metysova, J. Med. Pharm. Chem. 4 (1961) 411.
[17] H. Bönnemann, R. Brinkmann, W. Brijoux, E. Dinjus, Th. Joussen, B. Korall, Angew. Chem. 103 (1991) 1344.
[18] H. Bönnemann, W. Brijoux, A. Schulze Tilling, K. Siepen, Top. Catal. 4 (1997) 217.
[19] H. Bönnemann, U. Endruschat, B. Tesche, A. Rufínska, C.W. Lehmann, F.E. Wagner, G. Filoti, V. Pârvulescu, V.I. Pârvulescu, Eur. J. Inorg. Chem. (2000) 819.
[20] T. Komaya, A.T. Bell, Z.W. Sieh, R. Gronsky, F. Engelke, T.S. King, M. Pruski, J. Catal. 150 (1994) 400.
[21] D.O. Uner, M. Pruski, T.S. King, J. Catal. 156 (1995) 60.
[22] W. Treibs, H.J. Klinkhammer, Chem. Ber. 84 (1951) 671; W. Treibs, H.J. Klinkhammer, Chem. Ber. 83 (1950) 367.
[23] P. Debye, H.R. Anderson Jr., H. Brumberger, J. Appl. Phys. 28 (1957) 679.
[24] L. Guczi, R. Sundarajan, Zs. Koppany, Z. Zsoldos, Z. Schay, F. Mizukami, S. Niwa, J. Catal. 156 (1994) 60.